Photoionization of adsorbates on sites with non-axial local symmetry. An example of the C_{4v} symmetry group

1996 J. Phys.: Condens. Matter 8 10327

(http://iopscience.iop.org/0953-8984/8/49/023)

J. Phys.: Condens. Matter **8** (1996) 10327–10345. Printed in the UK

Photoionization of adsorbates on sites with non-axial local symmetry. An example of the C_{4v} symmetry group

V V Kuznetsov†, N A Cherepkov‡§ and G Raseev‖

† State Academy of Aerospace Instrumentation, 190000 St Petersburg, Russia
‡ Institut für Physik, Universität Mainz, 55099 Mainz, Germany
‖ Laboratoire de Photophysique Moleculaire du CNRS, Bâtiment 213, Campus d'Orsay, Université de Paris-Sud, 91405 Orsay, France

Received 29 April 1996, in final form 29 July 1996

Abstract. We present an analysis of the influence of the C_{4v} local adsorption site symmetry on the angular distribution of photoelectrons ejected from adsorbed atoms or molecules. This analysis applies to photoelectron spectra obtained with photons of any energy in the VUV (photoelectron spectroscopy) or x-ray (XPS) regions, provided that the associated wave of the electron 'sees' the neighbouring surface atoms. The adsorbate–substrate system is modelled by a cluster of C_{4v} symmetry group consisting of an adsorbate and several atoms of the substrate. The analysis applies also to clean surfaces of C_{4v} symmetry and to molecules of the C_{4v} symmetry group fixed in space. This local symmetry analysis is an alternative to models of photoelectron diffraction and backscattering of photoelectrons from the surface. To unravel specific symmetry properties of the system we use the expansion of continuous spectrum wavefunctions in symmetry-adapted harmonics instead of expansion in spherical harmonics. The particular cases of circularly and linearly polarized light beams incoming along the C_4 rotation axis are considered. Terms appearing in the analytical expressions for the differential cross section and for linear or circular dichroism in the angular distribution of photoelectrons are either common to C_{4v} and axial symmetry groups $C_{\infty v}$ and $D_{\infty h}$ or specific to the C_{4v} group. The presence of the latter terms allows identification of the symmetry of the adsorption site and the position of the molecule on the surface. We illustrate the analytical expressions by modelling the CO molecule adsorbed on a Ni(100) surface.

1. Introduction

Photoelectron spectroscopy is a powerful method of experimental investigation of the interaction between adsorbed molecules and surfaces and of the geometry of the adsorbate–substrate system. Evidently, the most detailed information on the system under consideration can be obtained from angle- and spin-resolved photoelectron spectroscopy in the VUV or x-ray excitation energy regions. The spin polarization measurements are rather complicated and as a consequence scarce, but even measurements of the angular distributions of photoelectrons without spin analysis are very informative. One can have an idea of the orientation of adsorbed molecules towards the surface by a combination of measurements of the angular distributions of photoelectrons ejected from adsorbed molecules [1] and theoretical calculations [2–4].

In many theoretical investigations, an adsorbed molecule was considered as an isolated object fixed in space and the influence of the surface was neglected [2–5]. In the simplest

§ Permanent address: State Academy of Aerospace Instrumentation, 190000 St Petersburg, Russia.

0953-8984/96/4910327+19$19.50

model for an adsorbed atom the influence of the surface was described by introducing a non-isotropic initial state wavefunction corresponding to the local chemical bond structure [6]. This allowed one to describe (at least partially) the local symmetry of the surface. The chemical bond of an adsorbed molecule in the on-top position was introduced through a model of a linear cluster including a single atom of the surface. The initial and final states were considered on an equal footing and included the chemical bond with the surface atom. The associated calculations, of Xα [7] or *ab initio* types [8], considered the surface as a structureless plane, neglecting its local symmetry. In [9] calculations for a molecule fixed in space and in [10] for a linear cluster including one atom from the surface were performed with addition of the backscattering effects from a step potential representing the structureless surface.

In a different approach the backscattering of photoelectrons from surrounding atoms of the substrate was explicitly included [11–14] and in this way the local symmetry of the surface was properly taken into account. However, the initial state effects were neglected (which is justified for inner-shell ionization) in this approach. In calculations of this type it is difficult to obtain the analytical expressions for the angular distributions and the general conclusions are usually drawn from the results of numerical calculations. The backscattering from the structureless potential step applies to photoelectrons of low kinetic energy, at which elementary processes correspond to multiple scattering from the surrounding atoms. In other words the associated de Broglie wave of the electron spreads over several atoms of the surface. At moderate and high kinetic energies single scattering prevails, the wavelength of the electron is shorter than the size of the elementary cell and the electron 'sees' the target atoms individually. From the very beginning [6, 11] it was clear that the influence of the surface symmetry, appearing through chemical bonding and photoelectron backscattering, is important when the kinetic energy of the electrons is sufficiently high and that this symmetry should be taken into account.

The purpose of the present paper is to investigate analytically at a qualitative level the influence of the local symmetry of the adsorption site on the angular distribution of photoelectrons ejected by circularly and linearly polarized light. We model the photoionization of an adsorbate by considering the photoionization of a cluster consisting of an adsorbed atom or molecule and several atoms of a substrate arranged to fulfil the symmetry of the adsorption site. This is an alternative way to describe the diffraction of photoelectrons from the nearest neighbours considered in [11–14]. To unravel the specific symmetry properties of the system without cumbersome calculations, we expand continuous spectrum wavefunctions in symmetry-adapted harmonics [15], as was proposed in [16–18], instead of expanding in spherical harmonics as has been done previously [2–4]. The use of a model cluster for the calculations enables one to take into account both initial and final states effects simultaneously, including the backscattering from atoms of the first (or several, depending on the size of the cluster) co-ordination sphere. The translational periodicity of the target and the scattering and diffraction from atoms beyond the cluster are neglected in this model, so that some purely solid state effects are disregarded.

A theoretical model that unravels at quantitative level the complete local symmetry should fulfil two conditions. First, as is done in this paper, the cross section should be written taking into account explicitly the symmetry constraints of the local symmetry of the surface. Secondly, the transition probability from the initial to the final state has to be calculated taking into account fully the symmetry and the interactions of the adsorbate–substrate system. Here we do not calculate these transition probabilities explicitly but instead treat them as adjustable parameters. Particularly in the example presented below, we consider the adsorption of $c(2\times 2)$ CO molecules on a Ni(100) surface (see figure 1) that corresponds to the C_{4v} local symmetry group. Horn *et al* [19c] have shown that the correct

crystallographic notation for the structure of the adsorbed CO is $(\sqrt{2} \times \sqrt{2})$ R45° (the full square in figure 1). Here we are interested in the local symmetry about the on-top adsorption site that is easily seen by using $c(2 \times 2)$ notation (the broken square in figure 1). We adopt this latter notation in the present paper. From several experiments [19] it follows that, at a temperature of around 300 K and a coverage of about 0.5 of a monolayer, the $c(2 \times 2)$ CO molecules are located in on-top sites (nearly) normal to the surface with the O atom pointing towards the vacuum (figure 2). They form together with five nearest neighbour atoms a cluster of C_{4v} symmetry. Evidently, one can include also more than five atoms from the substrate provided that the C_{4v} symmetry of the cluster is maintained. The model developed in this paper can also be applied to C_{4v} molecules adsorbed on surfaces (on any surfaces if the interaction with the surface is weak, or on C_{4v} surfaces otherwise) and to clean surfaces of the same symmetry.

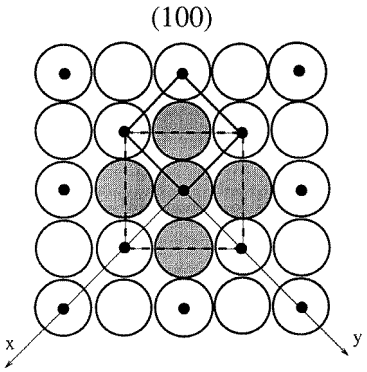

Figure 1. The view from above of the on-top adsorption of CO on a Ni(100) surface. Large unfilled circles are Ni atoms and small full circles are the CO molecules. Andersson and Pendry [19a] draw a $c(2 \times 2)$ adsorption structure (broken square) that shows the C_4 local symmetry. It does not correspond to the simplest structure constructed from the elementary cell of the adsorbate substrate system. This structure (the full square in the figure), given in the paper by Horn *et al* [19c], is $(\sqrt{2} \times \sqrt{2})$ R45°. The on-top position of the CO molecule represented in figure 2 displays the four filled Ni atoms and the central one together with the x and y axes of the coordinate system.

In photoionization of adsorbed molecules the general theoretical expressions for angular distributions of photoelectrons are usually fairly complicated. Only rarely can one extract qualitative information on the orientation of adsorbed molecules or on adsorbate–substrate interaction from the experimental data. Instead of the angular distribution itself, one can determine differences between angular distributions with two light polarizations. These differences, known as dichroism in the angular distribution of photoelectrons, are called circular dichroism in the angular distribution (CDAD) for left- and right-circular polarization of light, whereas using two mutually perpendicular linear polarizations one measures linear dichroism in the angular distribution (LDAD). In particular, for diatomic molecules standing normal to the structureless surface one finds non-zero CDAD if the directions of the incident light, of the molecular axis and of the momentum of ejected electron are not coplanar [5, 9, 10]. Here our surface has C_4 local symmetry and we will show that there is non-zero dichroism for the three vectors mentioned above coplanar. Moreover, for particular directions of the vectors characterizing the process and independently from the incident photon energy, one finds zeros in the dichroism. These zeros help in the qualitative analysis of the geometry of the adsorbed system and of its interactions.

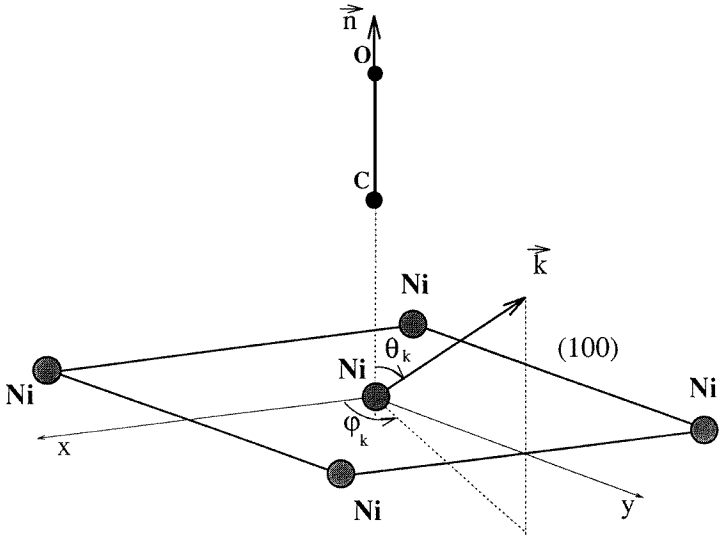

Figure 2. A three-dimensional representation of a cluster consisting of a CO molecule adsorbed normal to the surface above a Ni atom (in the on-top position) and four nearest neighbouring Ni atoms fulfilling the C_{4v} local symmetry in the geometrical arrangement of figure 1. The co-ordinate system having its z axis normal to the surface ($z \| \boldsymbol{n}$) is also shown.

The appearance of CDAD for achiral (linear in particular) molecules fixed in space was first predicted in [20] and later discussed in more detail in [5, 21–23]. The experimental investigations with adsorbed molecules [24] demonstrated that CDAD can be easily observed and used, for example, to determine the molecular orientation. The first consideration of CDAD from nonlinear molecules using expansion in symmetry-adapted harmonics was presented in [25]. The appearance of LDAD for molecules fixed in space was predicted more recently [26] and there have been calculations [23, 27] and measurements [28] for adsorbed linear molecules. Here, for the first time, we derive both the CDAD and the LDAD for the C_{4v} symmetry group of adsorbate–substrate systems or oriented molecules and discuss their characteristic angular behaviour.

The above presentation neglected internal and collective vibrations of adsorbed molecules. This motion can destroy the local symmetry of the adsorbate–substrate system and cause a smoothing of spectra. The hindered rotation of the adsorbed molecule should be singled out from the other nuclear motions since it modifies the direction of the molecular axis (which is considered to be fixed in this paper) and influences directly the angular distribution of photoelectrons [29]. Below, it is assumed that the molecule is standing upright on the surface. However, often the molecule seems to be slightly tilted with an angle of 5–15° to the normal [30, 31] (sometimes the estimation is higher [32]) and precessing about the surface normal.

Another point discarded in this paper is the coverage of the surface by the adsorbate. Studies of the spectra of adsorbates for different coverages reveal that the molecular axis of the adsorbate is tilted. Also when increasing the coverage the molecules are adsorbed on different adsorption sites (depending on the metallic substrate the adsorption is first on-top then bridge and finally three-fold hollow or reverse). These modifications are due to adsorbate–adsorbate interaction and have been taken into account in [33].

2. Angular distributions of photoelectrons

In 1976 Dill [2] was the first to derive general expressions for the angular distribution of photoelectrons (ADP) ejected from molecules of arbitrary symmetry fixed in space. Later these expressions were generalized [5] to include photoelectron spin and were specified [5, 16] for particular symmetry groups. In these derivations the vibrational degrees of freedom were not considered explicitly but they can be easily taken into account provided that they do not modify the direction of the main molecular axis as does libration or hindered rotation [29].

The formulae derived below do not include spin explicitly but are otherwise general. To be specific we will refer in the following to an on-top adsorption of a diatomic molecule such that the local symmetry of the system under study is C_{4v}. We consider a photoelectron wavefunction ${}^{p}\psi^{-}_{\boldsymbol{k}}(\boldsymbol{r})$ normalized with respect to an energy delta function and constructed in the asymptotic region from a superposition of a plane wave propagating in the direction of the electron momentum $\boldsymbol{k}$ and a converging spherical wave. In [2–5] this wavefunction has been expanded in spherical harmonics $Y_{\ell m}(\hat{\boldsymbol{k}})$ of the direction $\boldsymbol{k}$ for a photoelectron momentum $\boldsymbol{p}(\boldsymbol{k} = \boldsymbol{p}/p)$:

$$ {}^{p}\psi^{-}_{\boldsymbol{k}}(\boldsymbol{r}) = \sum_{\ell m} Y^{*}_{\ell m}(\hat{\boldsymbol{k}})\, {}^{p}\mathcal{F}_{\ell m}(\boldsymbol{r}) \tag{1} $$

where p is an irreducible representation (IR) of this function, $\boldsymbol{r}$ is the radius vector of the photoelectron in the molecular frame defined by the Z axis parallel to the C_4 rotational axis, with the X and Y axes lying in the planes of symmetry of the surface. ${}^{p}\mathcal{F}_{\ell m}$ is the complex channel function corresponding to an angular momentum ℓ and the energy $E = k^2/2$ (atomic units $\hbar = e = m = 1$ are used in this paper). The channel function can be further expanded in spherical harmonics of the $\boldsymbol{r}$ vector [34].

The expansion (1) does not reflect explicitly the local symmetry of the molecule–adsorbate system. This symmetry will appear only when performing a calculation and one will realize that some ${}^{p}\mathcal{F}_{\ell m}$ functions or components of these functions are zero. Then the calculation and the qualitative analysis are cumbersome. For molecule–adsorbate systems belonging to a given symmetry group it is more convenient to expand the wavefunctions not in spherical harmonics but rather in symmetry-adapted harmonics appropriate for the symmetry group of adsorbate–substrate system. The appropriate symmetry functions and their expansions in spherical harmonics have been defined in [35]. The use of these angular functions was proposed in the molecular studies by Burke *et al* [15] and Chandra [16]. This change in the angular basis enables one to investigate in a straightforward way those angular properties of the ADP, CDAD and LDAD that are independent of energy. Instead of (1) one writes the symmetry-adapted expression for the wavefunction as:

$$ {}^{p}\psi^{-}_{\boldsymbol{k}}(\boldsymbol{r}) = \sum_{\ell h \tau} {}^{p}\chi^{\tau *}_{h\ell}(\hat{\boldsymbol{k}})\, {}^{p}F^{\tau}_{h\ell}(\boldsymbol{r}) \tag{2} $$

where again p is an irreducible representation (IR) of this function. h and τ label the different functions of the same IR and the degeneracy of the IR, if any. The symmetry-adapted harmonics χ defined by Altmann *et al* [35] for several symmetry groups are linear combinations of the usual spherical harmonics:

$$ {}^{p}\chi^{\tau}_{h\ell}(\hat{\boldsymbol{k}}) = \sum_{m} {}^{p}b^{h\tau}_{\ell m} Y_{\ell m}(\hat{\boldsymbol{k}}) \tag{3} $$

where ${}^{p}b^{h\tau}_{\ell m}$ are the expansion coefficients. Table 1 contains these coefficients for the C_{4v} symmetry group restricted to the IR corresponding to the allowed transitions from the a_1

orbital in the case of A_1 initial state. For linearly polarized light the possible IRs of the final state orbitals are a_1 (z dipole transition; light is polarized parallel to the molecular axis $\boldsymbol{n}$) and e (x and y transitions; light is polarized perpendicular to this axis). Using the expressions (1)–(3) for the photoelectron wavefunctions and the results from [5] for the ADP of adsorbed molecules, one finds the expression for the intensity in the laboratory (where the z axis is parallel to the surface normal) or molecular frames (in which the z axis is parallel to the principal axis of the molecule) valid both for linearly and for circularly polarized light:

$$I^{m^{ph}}(\boldsymbol{k},\boldsymbol{e}) = \sigma_k(E)\sum_{J}^{2}\sum_{M_J}(1)^{1-m^{ph}}\sqrt{3}\begin{pmatrix}1 & 1 & J\\ -m^{ph} & m^{ph} & 0\end{pmatrix} \times \sum_{m_1^\gamma m_2^\gamma}\frac{\sqrt{3}}{B}[J]^{1/2}(-1)^{m_1^\gamma+1}\begin{pmatrix}1 & 1 & J\\ -m_1^\gamma & m_2^\gamma & M_J\end{pmatrix}K(m_1^\gamma,m_2^\gamma,\hat{\boldsymbol{k}})Y_{JM_J}(\hat{\boldsymbol{e}}). \quad (4)$$

Here $\boldsymbol{e}$ is the polarization vector for linearly polarized light with projection m^{ph} in the photon frame equal to zero. The above equation applies also for circularly polarized light provided that the vector $\boldsymbol{e}$ is replaced by the unit vector $\boldsymbol{q}$ in the direction of the light beam with the projection of the light angular momentum $m^{ph} = \pm 1$. Note that in (4) we used the notation $[J] = 2J + 1$. The orientation of $\boldsymbol{e}$ and $\boldsymbol{q}$ about the reference frame (molecular or laboratory) is given by θ_q and φ_q. Now $K(m_1^\gamma, m_2^\gamma, \boldsymbol{k})$, $\sigma(E)$ and B have the following analytical expressions:

$$K(m_1^\gamma,m_2^\gamma,\hat{\boldsymbol{k}}) = \sum_{\substack{\ell_1\ell_2\\ L}}\sum_{\substack{h_1\tau_1\\ h_2\tau_2}}\langle 0|\hat{d}^*_{m_1^\gamma}|\,{}^pF^{\tau_1}_{h_1\ell_1}(\boldsymbol{r})\rangle\langle\,{}^pF^{\tau_2}_{h_2\ell_2}(\boldsymbol{r})|\hat{d}_{m_2^\gamma}|0\rangle \times \sum_{\substack{m_1,m_2\\ M_L}}{}^pb^{h_1\tau_1^*}_{\ell_1 m_1}\,{}^pb^{h_2\tau_2}_{\ell_2 m_2}(-1)^{m_2}\begin{pmatrix}\ell_1 & \ell_2 & L\\ 0 & 0 & 0\end{pmatrix} \times\begin{pmatrix}\ell_1 & \ell_2 & L\\ -m_1 & m_2 & -M_L\end{pmatrix}[\ell_1,\ell_2,L]^{1/2}Y_{LM_L}(\hat{\boldsymbol{k}}) \quad (5)$$

$$\sigma(E) = \frac{4\pi^2\alpha E}{3n_g}B \quad (6a)$$

$$B = \sum_{ds}\sum_{\ell,m,m^\gamma}|\langle 0|\hat{d}^*_{m^\gamma}|\,{}^p\mathcal{F}_{\ell m}(\boldsymbol{r})\rangle|^2 = \sum_{ds}\sum_{h,\ell,\tau,m^\gamma}|\langle 0|\hat{d}^*_{m^\gamma}|\,{}^pF^{\tau}_{h\ell}(\boldsymbol{r})\rangle|^2. \quad (6b)$$

Here α is the fine-structure constant, E the photon energy, n_g the statistical weight of the initial state. The expressions (4) and (6) contain a sum over all degenerate final states of the different IRs accessible by photoionization. In expression (6*b*), B is a sum of squares of transition moments written for an orthonormal basis $Y_{\ell m}(\hat{\boldsymbol{k}})$ of (1) or $\chi_k(\hat{\boldsymbol{k}})$ of (2). If one uses the Altmann and Bradley [35] tables in which the functions are not normalized, then one has to multiply each transition moment by an appropriate normalization constant. The integral $\langle F|d|0\rangle$ is the one-electron transition moment. For an adsorbate–substrate model cluster of N electrons this integral should be replaced by:

$$\langle\det({}^{p_i}\psi(1,2,\ldots N-1)\,{}^pF^{\tau}_{h\ell}(\boldsymbol{r}_N))|\hat{d}_{m^\gamma}|\,{}^{p''}\psi(1,2,\ldots N)\rangle \cong \langle\,{}^pF^{\tau}_{h\ell}(\boldsymbol{r})|\hat{d}_{m^\gamma}|0\rangle. \quad (7)$$

The expression (7) reduces to the one-electron matrix element appearing in (5) and (6*b*) when the wavefunctions for the initial and final states are written as single electronic configurations with a unique orthonormal basis. If multiconfiguration functions for the initial and final states are introduced then in the most general case several one-electron functions ${}^pF^{\tau}_{h\ell}(\boldsymbol{r})$

Table 1. Symmetry-adapted spherical harmonics for the C_{4v} symmetry group. This table is written for the photoionization from a totally symmetrical A_1 state. The dipole-selection rules restrict the possible final states to A_1 and E. Tables including all the irreducible representations have been given by Altmann *et al* [35]. We use complex normalized symmetry-adapted spherical harmonics. Altmann *et al* [35] used unnormalized real harmonics defined as follows: $Y^c_{\ell m}(\theta,\varphi) = P_{\ell m}(\cos\theta)\cos(m\varphi)$ and $Y^s_{\ell m}(\theta,\varphi) = P_{\ell m}(\cos\theta)\sin(m\varphi)$; here $P_{\ell m}(\cos\theta)$ is the usual Legendre polynomial.

IR	Indices				Symmetry-adapted	${}^p b^{h\tau}_{\ell m}$		
p	ℓ	h	τ	n	spherical harmonics	$-m$	0	m
A_1	$\geqslant 0$	1	1	0	$Y_{\ell 0}$		1	
	$\geqslant 4$	$\geqslant 2$	1	$\geqslant 1$	$\frac{1}{\sqrt{2}}(Y_{\ell,-4n} + Y_{\ell,4n})$	$\frac{1}{\sqrt{2}}$		$\frac{1}{\sqrt{2}}$
E	$\geqslant 1$	$1, 3\ldots$	1	$\geqslant 0$	$\frac{1}{\sqrt{2}}(Y_{\ell,-1-4n} - Y_{\ell,1+4n})$	$\frac{1}{\sqrt{2}}$		$-\frac{1}{\sqrt{2}}$
	$\geqslant 3$	$2, 4\ldots$	1	$\geqslant 0$	$\frac{1}{\sqrt{2}}(Y_{\ell,-3-4n} - Y_{\ell,3+4n})$	$\frac{1}{\sqrt{2}}$		$-\frac{1}{\sqrt{2}}$
	$\geqslant 1$	$1, 3\ldots$	2	$\geqslant 0$	$-\frac{1}{\sqrt{2}}(Y_{\ell,-1-4n} + Y_{\ell,1+4n})$	$-\frac{1}{\sqrt{2}}$		$-\frac{1}{\sqrt{2}}$
	$\geqslant 3$	$2, 4\ldots$	2	$\geqslant 0$	$\frac{1}{\sqrt{2}}(Y_{\ell,-3-4n} + Y_{\ell,3+4n})$	$\frac{1}{\sqrt{2}}$		$\frac{1}{\sqrt{2}}$

of different IRs p of the excited electron give a contribution to the transition moments appearing in (5) and (6).

3. The particular case of the light beam parallel to the molecular axis

As a specific example of the equations (4)–(7), we consider below the CO molecule adsorbed on a Ni(100) surface in the $c(2\times 2)$ symmetry arrangement. The molecule and the atoms in the first co-ordination sphere fulfil the C_{4v} local symmetry (see figures 1 and 2). Let the light be linearly polarized along the [100] direction. As discussed above in relation to equation (3), the valence photoionization occurs by excitation of a valence electron from the a_1 orbital to a_1 or e continua. Using the formulae (4)–(7) and table 1, one finds the following differential cross section:

$$I^0(\boldsymbol{k},\varepsilon\|OX) = \frac{3\sigma_k(E)}{4\pi B}\{\mathrm{Re}(D_2(\theta_k))\sin^2\theta_k[1+\cos(2\varphi_k)] + \mathrm{Re}(D_4(\theta_k))\sin^4\theta_k[\cos(2\varphi_k) + \cos(4\varphi_k)] + D_6(\theta_k)\sin^6\theta_k[1+\cos(6\varphi_k)]\} \tag{8}$$

where θ_k and φ_k are the spherical angles of the vector $\boldsymbol{k}$ in the molecular frame (see figure 2),

$$\begin{aligned} D_2(\theta_k) = {} & \frac{3}{2}|\langle 0|x|{}^eF^1_{11}\rangle|^2 + 3\sqrt{5}\cos\theta_k\langle 0|x|{}^eF^1_{11}\rangle\langle {}^eF^1_{12}|x|0\rangle \\ & + \frac{15}{2}\cos^2\theta_k|\langle 0|x|{}^eF^1_{12}\rangle|^2 + \frac{3\sqrt{7}}{2\sqrt{2}}(5\cos^2\theta_k - 1)\langle 0|x|{}^eF^1_{11}\rangle\langle {}^eF^1_{13}|x|0\rangle \\ & + \frac{3\sqrt{35}}{2\sqrt{2}}\cos\theta_k(5\cos^2\theta_k - 1)\langle 0|x|{}^eF^1_{12}\rangle\langle {}^eF^1_{13}|x|0\rangle \\ & + \frac{21}{16}(5\cos^2\theta_k - 1)^2|\langle 0|x|{}^eF^1_{13}\rangle|^2 \end{aligned} \tag{9a}$$

$$\begin{aligned} D_4(\theta_k) = {} & \frac{\sqrt{105}}{2\sqrt{2}}\langle 0|x|{}^eF^1_{11}\rangle\langle {}^eF^1_{23}|x|0\rangle + \frac{5\sqrt{21}}{2\sqrt{2}}\cos\theta_k\langle 0|x|{}^eF^1_{12}\rangle\langle {}^eF^1_{23}|x|0\rangle \\ & + \frac{7\sqrt{15}}{8}(5\cos^2\theta_k - 1)\langle 0|x|{}^eF^1_{13}\rangle\langle {}^eF^1_{23}|x|0\rangle \end{aligned} \tag{9b}$$

$$D_6 = \frac{35}{16}|\langle 0|x|^e F^1_{23}\rangle|^2 \tag{9c}$$

$$B = |\langle 0|z|^a F^1_{10}\rangle|^2 + |\langle 0|z|^a F^1_{11}\rangle|^2 + |\langle 0|z|^a F^1_{12}\rangle|^2 + |\langle 0|z|^a F^1_{13}\rangle|^2 + 2|\langle 0|x|^e F^1_{11}\rangle|^2 + 2|\langle 0|x|^e F^1_{12}\rangle|^2 + 2|\langle 0|x|^e F^1_{13}\rangle|^2 + 2|\langle 0|x|^e F^1_{23}\rangle|^2. \tag{10}$$

In expressions (8)–(10) we used the real transition operators $\boldsymbol{x}$, $\boldsymbol{y}$ and $\boldsymbol{z}$ instead of the complex ones $\hat{d}_{m^\gamma}$ defined in (5). Due to the presence of reflection planes of the C_{4v} symmetry group the following relations hold between the transition moments:

$$\langle 0|x|^e F^\tau_{hl}\rangle = \mathrm{i}\langle 0|y|^e F^\tau_{hl}\rangle. \tag{11}$$

In the expression (9) and (10) we have restricted the expansion of the wavefunction (2) to $\ell \leqslant 3$. This is because we are keeping in mind the shape resonances (5σ and 4σ) in the CO molecule in which the main partial waves contributing to the differential cross section are lower or equal to three. With this restriction in the wavefunction expansion (1) or (2) one can still reveal contributions specific to the C_{4v} symmetry group. The transitions to the final states corresponding to an IR with $h = 1$ appear both for axial ($C_{\infty v}$ and $D_{\infty h}$ symmetry groups) and for C_{4v} symmetries whereas transitions to the final states with $h = 2$ correspond to C_{4v} symmetry only. In (8) and (9) the coefficients D_4 and D_6 are non-zero only for adsorbate–substrate local symmetry C_{4v} whereas the D_2 coefficient appears already for axial symmetry.

The angular dependence of the intensity (8) for the light polarized along the x axis (in the [100] crystallographic direction) has some characteristic features independent from a particular molecule or photon energy. Since the photoelectron current is proportional to $\sin^2\theta_k$, it goes to zero for photoelectrons ejected along the z laboratory axis. For the CO molecule adsorbed on metallic substrates at low coverage, this coincides with the adsorbate's molecular axis. It is also equal to zero in the plane perpendicular to the light polarization vector, that is in the YOZ plane (see figure 2) where $\varphi_\kappa = \pi/2$ or $3\pi/2$. The terms containing the fourfold dependence ($\cos(4\varphi_\kappa)$) appear in (8) together with the terms containing $\cos(2\varphi_\kappa)$ and $\cos(6\varphi_\kappa)$. The latter terms appear due to the presence of the light polarization vector $\boldsymbol{e}$ in the plane perpendicular to the C_4 rotation axis that makes the directions along the x and y axes inequivalent.

The $\cos(n\varphi_\kappa)$ behaviour of the photoionization cross section is related to the local symmetry of the surface and consequently is valid also for clean surfaces. Obviously when an adsorbate is present it should not lower the local symmetry of the overall system. For C_{4v} local symmetry of the adsorbate–substrate systems, one can easily test the $\cos(4\varphi_\kappa)$ behaviour by changing the azimuthal collection angle of the ejected photoelectron. This has been observed experimentally [19d] but the accuracy of the data was insufficient to extract the fourfold symmetry behaviour in the cross section unambiguously.

To show the behaviour of the angular distribution as a function of the angles φ_κ and θ_κ we performed a model calculation in which we used the following numerical values of the transition moments' moduli:

$$|\langle 0|x|^e F^1_{11}\rangle| \equiv d_{11} = 0.4 \qquad |\langle 0|x|^e F^1_{12}\rangle| \equiv d_{12} = 0.6$$
$$|\langle 0|x|^e F^1_{13}\rangle| \equiv d_{13} = 1.0 \qquad |\langle 0|x|^e F^1_{23}\rangle| \equiv d_{23} = 0.6 \tag{12a}$$

and their corresponding phases:

$$\delta_{11} = 1.1 \qquad \delta_{12} = 2.8$$
$$\delta_{13} = 1.9 \qquad \delta_{23} = 0.44. \tag{12b}$$

The ratios among the d_{11}, d_{12} and d_{13} transition matrix elements which have counterparts in linear molecules are chosen to be equal to the corresponding ratios of the transition moments in the maximum ($h\nu = 36$ eV) of the shape resonance in the ionization of the 4σ orbital of the CO molecule [9]. The phase shifts were also taken from [9]. The modulus of the transition moment d_{23} was chosen to be of the same order of magnitude as the other transition moments in equation (12*a*). The corresponding phase shift was chosen to give non-zero differences from the other phase shifts. All the transition moments of equation (12) were introduced in the expressions (8)–(11) above, for which the light beam is linearly polarized and propagates along the C_4 rotational axis. Our model case serves to illustrate the angular behaviour of photoelectron intensities only. Therefore in the following numerical example we omit the factor in front of the curly brackets in (8) containing the photoionization cross section that we have not calculated.

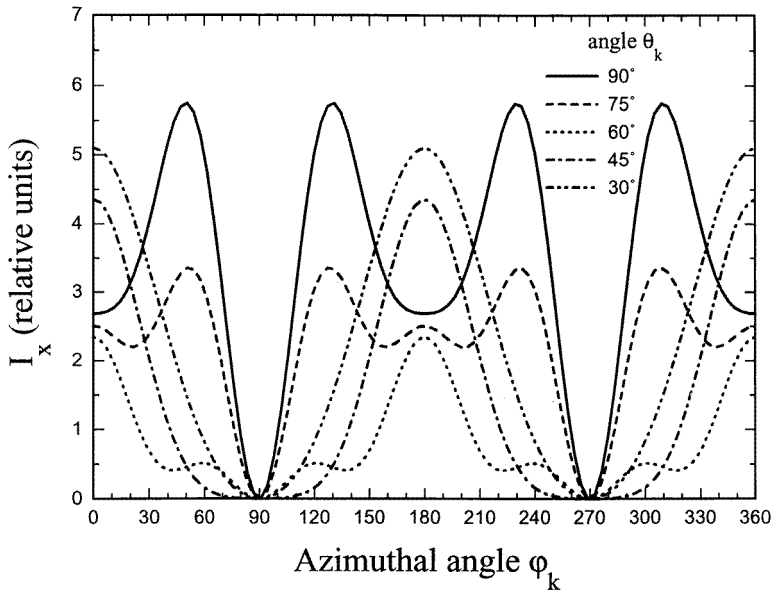

Figure 3. The differential photoelectron intensity I_x (the term in curly brackets of equation (8)) as a function of the photoelectron ejection azimuthal angle φ_k for several values of the polar angle θ_k. The light beam is incoming along the C_4 rotation axis of the molecule and is linearly polarized along the x axis of the molecular frame.

In figure 3 we display the dependence of the photoelectron intensity on the angle φ_κ for several values of the angle θ_k. At θ_k close to 90° the $D_2(\theta_k)$ and $\mathrm{Re}(D_4(\theta_k))$ terms in (8) are approximately equal and have opposite signs. As a result, the full curve in figure 3 showing the corresponding angular distribution is approximately a superposition of $\cos(2\varphi_\kappa)$ and $\cos(4\varphi_\kappa)$ functions with a clearly visible fourfold symmetry. Unfortunately, for these ejection angles of the photoelectron the measurements are difficult. The $D_6(\theta_k)$ term in (8) is always smaller than the above-mentioned terms. However, its contribution is clearly seen at $\theta_k = 60°$ and 75°. At small angles $\theta_k \leqslant 30°$ the term with $D_2(\theta_k)$ gives the predominant contribution. Since this is the only term appearing for linear molecules, the angular distribution for small angles θ_k behaves like it does in linear molecules and has two maxima at $\varphi_\kappa = 0°$ and 180° that coincide with the direction of light polarization. The last conclusion is valid for all molecules and does not depend on the photon energy. If in

the expansion of the wavefunction (2) terms with $l > 3$ were included, additional terms proportional to $\cos(2m\varphi_\kappa)$ with $m > 3$ would appear in the angular distribution (8). All these terms are connected with non-axial symmetry.

Since the values of the dipole matrix element d_{23} and phase shift δ_{23} are rather arbitrary, we performed a sample calculation for one angle of electron ejection $\theta_k = 75^\circ$ with several values of these parameters. The results are presented in figure 4 for I_x. First of all, the contribution of the term with $\cos(6\varphi_k)$, which is responsible for the maxima at 0° and 180°, is clearly visible only when $d_{23} = 0.6$ and $\delta_{23} = 0.44$. For $d_{23} = 0.3$ and $\delta_{23} = 0.44$ this contribution is already hardly visible, whereas for $d_{23} = 0.15$ and $\delta_{23} = 0.44$ even the term with D_4 in (8) is becoming small, so that the angular dependence is approaching that for linear molecules. At $\varphi_k = \pm 30^\circ$ and $\pi \pm 30^\circ$ all the curves have the same magnitude because for these angles both $\cos(2\varphi_k) + \cos(4\varphi_k)$ and $1 + \cos(6\varphi_k)$ are zero, and the only remaining term in (8) proportional to $\mathrm{Re}(D_2)$ does not depend on the dipole transition d_{23} (see equation (9*a*)). The values of I_x at $\varphi_k = 90^\circ$ and 270° are also fixed, therefore the curves of figure 4 represent practically all the possible dependences that can appear for this experimental geometry when $l \leqslant 3$.

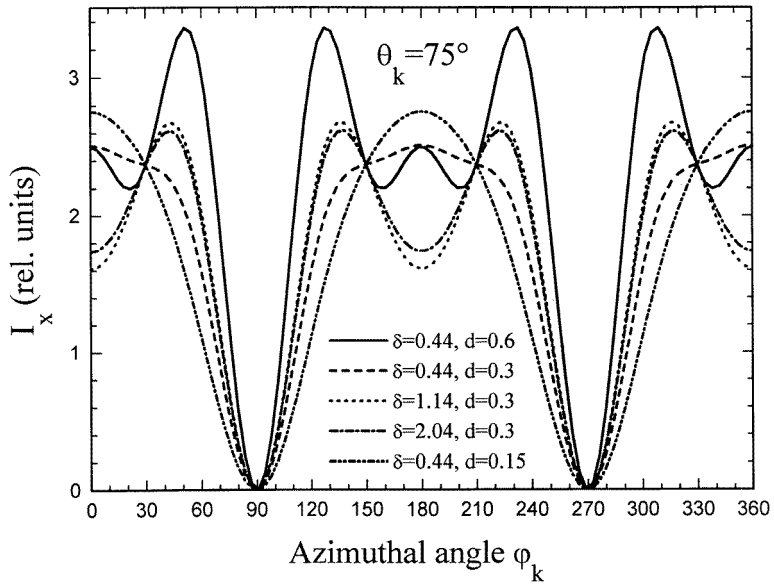

Figure 4. The same as in figure 3 but for $\theta_k = 75^\circ$ and different values of the transition matrix element d_{23} and the corresponding phase shift δ_{23} (see definition in equation (12)) listed in the figure.

Consider now an example of a circularly polarized light beam propagating along the C_4 rotational axis of molecules. The angular distribution of photoelectrons for absorption of left (+) or right (−) circularly polarized light reads:

$$I^{\pm}(\boldsymbol{k}, \boldsymbol{q} \| \boldsymbol{n}) = \frac{3\sigma_k(E)}{4\pi B}\{\mathrm{Re}(D_2(\theta_k))\sin^2\theta_k + \sin^4\theta_k \times [\mathrm{Re}(D_4(\theta_k))\cos(4\varphi_k) \pm \mathrm{Im}(D_4(\theta_k))\sin(4\varphi_k)] + D_6\sin^6\theta_k\}. \quad (13)$$

Compared to equation (8) for linearly polarized light, the terms with $\cos(2\varphi_\kappa)$ and $\cos(6\varphi_\kappa)$ have disappeared and only terms of fourfold symmetry proportional to $\cos(4\varphi_\kappa)$ and $\sin(4\varphi_\kappa)$

survive, together with the terms independent from φ_κ. This is because now the light beam has no characteristic direction in the surface plane perpendicular to the C_4 rotation axis. Equation (13) is again proportional to $\sin^2(\theta_k)$, therefore the photoelectron current is zero at $\theta_k = 0$ and π. The relatively simple structure of equation (13) is connected with our restriction in the expansion of the wavefunction (2) by the partial waves with $\ell \leqslant 3$. Inclusion of the partial wave with $\ell = 4$ will lead to the appearance of terms proportional to $\sin(8\varphi_\kappa)$ and $\cos(8\varphi_\kappa)$ in (13), and, as a consequence, to additional maxima and minima in the angular distributions. More generally, inclusion of terms with $l > 3$ will lead to the appearance of terms proportional to $\sin(4m\varphi_\kappa)$ and $\cos(4m\varphi_\kappa)$ with $m = 2, 3, \ldots$ in (13). In practice, however, it is reasonable to expect that the terms with $m \geqslant 3$ will be small.

In figure 5 we illustrate the dependence of the photoelectron intensity I^+ on the angle φ_κ for several values of the angle θ_k and for the transition moments defined in (12). The positions of maxima strongly depend on the angle θ_k and they are much more pronounced for angles θ_k close to 90°. Evidently, the positions of maxima depend on the matrix elements and phase shifts and will vary with photon energy. To demonstrate the dependence of the angular distribution I^+ on the values of the matrix element d_{23} and the phase shift δ_{23} we performed again calculations for different values of these parameters and a fixed value of the angle $\theta_\kappa = 75°$. They are presented in figure 6. Now the dependences on d_{23} and δ_{23} are rather systematic and simple. Namely, the curves obtained with a fixed value of $\delta_{23} = 0.44$ and decreasing magnitudes of d_{23} have the same positions of maxima and minima while the depth of modulation is decreasing. Variation of the phase δ_{23} for a fixed value of the matrix element d_{23} shifts the curve in the horizontal direction without any change in its magnitude.

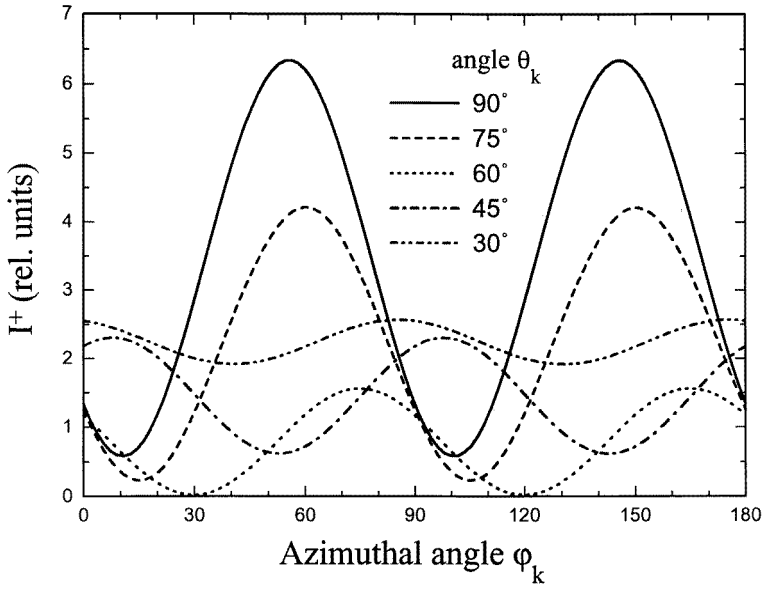

Figure 5. Differential photoelectron intensities I^+ for left-circularly polarized light (equation (13)). The notations are the same as in figure 3.

When the light polarization is changed from left- to right-circularly polarized, the terms with $\sin(4m\varphi_\kappa)$ in (13) change in sign while the signs of the terms with $\cos(4m\varphi_\kappa)$ remain unchanged. The corresponding curves for the angular distributions for opposite light

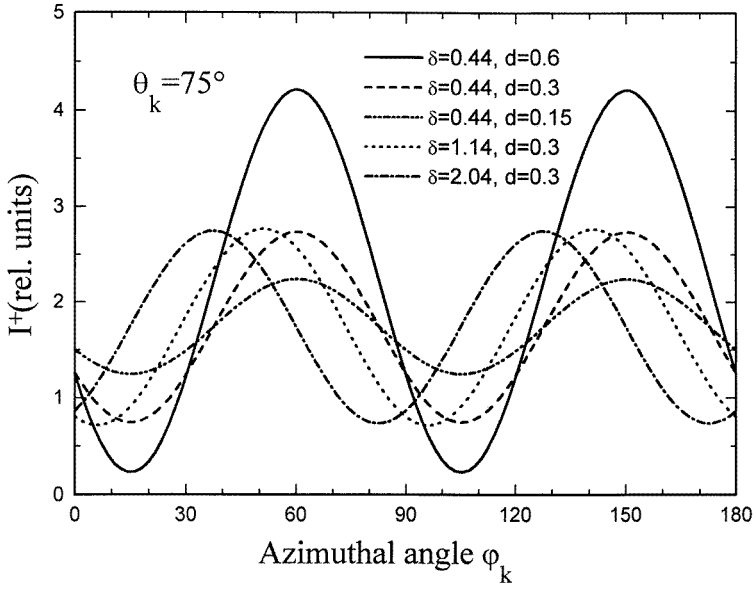

Figure 6. The same as in figure 4 but for $\theta_k = 75^\circ$ and different values of the transition matrix element d_{23} and phase shift δ_{23} listed in the figure.

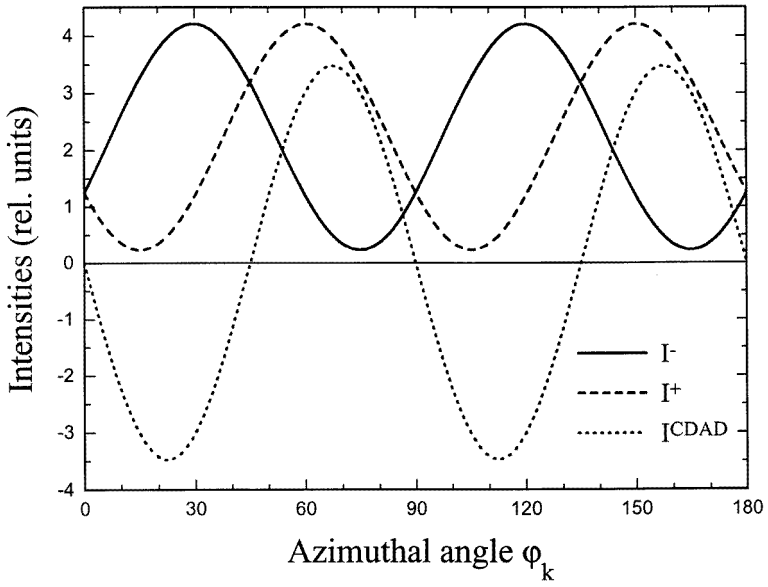

Figure 7. Photoelectron intensities $I^{\pm}$ (equation (13)) for left (broken curve) and right (full curve) circularly polarized light, and I^{CDAD} (dotted curve) for the electron ejection angle $\theta_k = 75^\circ$.

polarization can be obtained from one another by mirror reflection at the angles $\varphi_\kappa = 0^\circ$, 45°, $90^\circ \ldots$ as illustrated in figure 7.

4. Dichroism in the angular distribution of photoelectrons

The differential photoionization cross section gives the complete information about the system under consideration but this information is sometimes too rich to be interpreted qualitatively. For a particular experimental geometry, one obtains specific information by studying the circular (CDAD) and linear (LDAD) dichroisms in the angular distribution (see for example [5, 20–24, 26–28]). Let us start with CDAD that is a difference between the cross sections for left- and right-circularly polarized light. Using the expressions (4)–(7) for this particular situation, one obtains

$$\begin{aligned} I^{CDAD}(\boldsymbol{k},\boldsymbol{q}) = I^{+}(\boldsymbol{k},\boldsymbol{q}) - I^{-}(\boldsymbol{k},\boldsymbol{q}) = \frac{\sigma_k(E)}{B}\frac{3}{2\sqrt{\pi}}\{&\cos\theta_q[K(1,1,\hat{\boldsymbol{k}}) - K(-1,-1,\hat{\boldsymbol{k}})] \\ &+\sqrt{2}\sin\theta_q\cos\varphi_q \mathrm{Re}(K(-1,0,\hat{\boldsymbol{k}}) + K(0,1,\hat{\boldsymbol{k}})) \\ &+\sqrt{2}\sin\theta_q\sin\varphi_q \mathrm{Im}(K(-1,0,\hat{\boldsymbol{k}}) + K(0,1,\hat{\boldsymbol{k}}))\} \end{aligned} \tag{14}$$

where we have used the condition

$$K(m_1^{\gamma}, m_2^{\gamma}, \hat{\boldsymbol{k}}) = K^{*}(m_2^{\gamma}, m_1^{\gamma}, \hat{\boldsymbol{k}}). \tag{15}$$

When in particular the circularly polarized light propagates along the C_4 symmetry axis and only terms with $\ell \leqslant 3$ are retained in the expansion (2), the resulting expression for I^{CDAD} is much simpler:

$$I^{CDAD}(\boldsymbol{k},\boldsymbol{q}\|\boldsymbol{n}) = -\frac{3\sigma_k(E)}{2\pi B}\mathrm{Im}(D_4(\theta_k))\sin^4\theta_k\sin(4\varphi_k). \tag{16}$$

For axially symmetrical adsorbate–substrate systems the above expression is identically zero because the three vectors describing the process, $\boldsymbol{n}$, $\boldsymbol{q}$ and $\boldsymbol{k}$, are coplanar [5, 21]. Therefore all the contributions to (16) are specific for C_{4v} symmetry and have a simple $\sin(4\varphi_\kappa)$ behaviour, as shown in figure 7. As a consequence of this behaviour, there are zeros in the CDAD which coincide with the symmetry planes of the system. This is a general property of CDAD independent of photon energy or molecule. The sign and the magnitude of the CDAD depend on the matrix elements and phase shifts and will vary with photon energy. When terms with $\ell \geqslant 4$ are included, the contributions of terms with $\sin(4m\varphi_\kappa)$, $m = 2, 3, \ldots$ also appear, leading to a more complicated dependence of the CDAD on the angle φ_κ.

Next, we consider the LDAD defined as the difference between angular distributions corresponding to two light beams with mutually orthogonal linear polarizations. For axially symmetrical systems, this dichroism was presented in [26] and studied in detail in [27]. As mentioned in [26, 27], the expression (4), in which the light polarization is directed along the z axis of the photon co-ordinate system, is inconvenient for the derivation of the LDAD. Instead one should use a photon co-ordinate system in which the light propagates along the z axis and the two orthogonal linear polarizations coincide with the x and y axes of this co-ordinate system. We refer to [27] for a detailed derivation and give here just the final expression for the differential cross section with light polarized in the x direction and the LDAD result. First, this differential cross section for systems of arbitrary symmetry is written in the notation of the present paper as

$$\begin{aligned} I_{e_x}(\boldsymbol{k},\boldsymbol{q}) = 3\sigma_k(E)\sum_{J,M_J}\sum_{m_1^{\gamma},m_2^{\gamma}}\frac{1}{B}[J]^{1/2}(-1)^{m_1^{\gamma}+1}\begin{pmatrix} 1 & 1 & J \\ -m_1^{\gamma} & m_2^{\gamma} & M_J \end{pmatrix} K(m_1^{\gamma}, m_2^{\gamma}, \hat{\boldsymbol{k}}) \\ \times\left\{\frac{1}{2\sqrt{\pi}}\delta_{J0}\delta_{M_J0} + \frac{1}{\sqrt{10}}Y_{JM_J}(\hat{\boldsymbol{q}})\delta_{J2}\delta_{M_J0} - \frac{\sqrt{3}}{4\sqrt{\pi}}\delta_{J2}\right. \end{aligned}$$

$$\times[D^J_{-M_J 2}(\varphi_q, \theta_q, \chi_q) + D^J_{-M_J-2}(\varphi_q, \theta_q, \chi_q)]\Big\}. \tag{17}$$

The photon angular behaviour of equation (17) is expressed using Wigner rotational functions $D^J_{M_J,M_{J'}}(\varphi_q, \theta_q, \chi_q)$ where φ_q, θ_q and χ_q, are the Euler angles describing the transformation from the laboratory to the photon frame. To express it in a form as simple as I^{CDAD} (see equation (16) above), we explicitly introduce in (17) the analytical form of the $D^J_{M_J,M_{J'}}$ Wigner functions. One obtains for the non-axial symmetry case the LDAD as the difference between the differential cross sections for light linearly polarized in the y and x directions:

$$\begin{aligned} I^{LDAD}(\boldsymbol{k}, \boldsymbol{q}) = I_{e_y}(\boldsymbol{k}, \boldsymbol{q}) - I_{e_x}(\boldsymbol{k}, \boldsymbol{q}) = \frac{3\sigma_k(E)}{(4\pi B)^{1/2}} \\ \times\Big\{\left(\frac{2}{3}\right)^{1/2} K(0,0,\hat{\boldsymbol{k}}) - \frac{1}{2}[K(1,1,\hat{\boldsymbol{k}}) + K(-1,-1,\hat{\boldsymbol{k}})]\sin^2\theta_q\cos(2\chi_q) \\ -\frac{1}{\sqrt{2}}\mathrm{Re}\{(K(-1,0,\hat{\boldsymbol{k}}) - K(0,1,\hat{\boldsymbol{k}}))\mathrm{e}^{-\mathrm{i}\varphi_q} \\ \times[\sin(2\theta_q)\cos(2\chi_q) - 2\mathrm{i}\sin\theta_q\sin(2\chi_q)]\} \\ -\mathrm{Re}[K(-1,1,\hat{\boldsymbol{k}})(\cos(2\chi_q)(1+\cos^2\theta_q)\mathrm{e}^{-2\mathrm{i}\varphi_q} - 2\cos\theta_q\sin(2\chi_q)\mathrm{e}^{2\mathrm{i}\varphi_q})]\Big\}. \end{aligned} \tag{18}$$

Compared to the equation (14) for the CDAD the LDAD equation (18) contains different trigonometric functions and includes a new angle χ_q.

As for CDAD (see equation (14) above), we can write a specific expansion for the LDAD when the incoming light beam is parallel to the surface normal ($\boldsymbol{q}\|\boldsymbol{n}\|C_4$) and the polarization vectors are parallel to the [100] and [010] crystallographic directions. This particular form of (18) reads:

$$\begin{aligned} I^{LDAD}(\boldsymbol{k}, \boldsymbol{q}\|\boldsymbol{n}) = \frac{3\sigma_k(\omega)}{2\pi B}[\mathrm{Re}(D_2(\theta_k))\sin^2\theta_k\cos(2\varphi_k) + \mathrm{Re}(D_4(\theta_k))\sin^4\theta_k\cos(2\varphi_k) \\ + D_6\sin^6\theta_k\cos(6\varphi_k)]. \end{aligned} \tag{19}$$

At first sight, it seems surprising that here we do not obtain, as for the CDAD expression (14), a $\cos(4\varphi_\kappa)$ angular dependence. Instead the angular dependence contains $\cos(2\varphi_\kappa)$ as for axially symmetrical systems together with a $\cos(6\varphi_\kappa)$-dependence.

This can be understood by realizing that the angular distribution for two orthogonal linear polarizations lying in the reflection planes of the C_{4v} symmetry group should coincide after a rotation by 90° about the C_4 symmetry axis, that is after a substitution of φ_κ by $\varphi_\kappa + 90°$. This substitution changes the signs of $\cos(2\varphi_\kappa)$ and $\cos(6\varphi_\kappa)$ while that of $\cos(4\varphi_\kappa)(\cos(2m\varphi_\kappa)$ with even m, $m = 2, 4, \ldots$ in the general case) remains unchanged. Consequently the terms with $\cos(4\varphi_\kappa)$ in the LDAD cancel out. So, for the light beam parallel to the C_4 rotational axis the CDAD but not the LDAD reveals the fourfold symmetry periodicity. Figure 8 shows the LDAD calculated for our numerical model defined in (12). Here again the deviation from the behaviour typical for linear molecules is most pronounced for the angles θ_k around 90°, for which the term with $\cos(6\varphi_\kappa)$ gives the predominant contribution. For small θ_k the contribution of the term with $D_6(\theta_k)$ tends to zero and we have the LDAD behaviour typical of linear molecules. Since $D_6(\theta_k)$ is simply proportional to the square of the matrix element (see (9*c*)) it is always positive and only its magnitude can vary with photon energy. Therefore the curves of figure 8 should not strongly depend on photon energy except for the magnitude of the modulation with $\cos(6\varphi_\kappa)$.

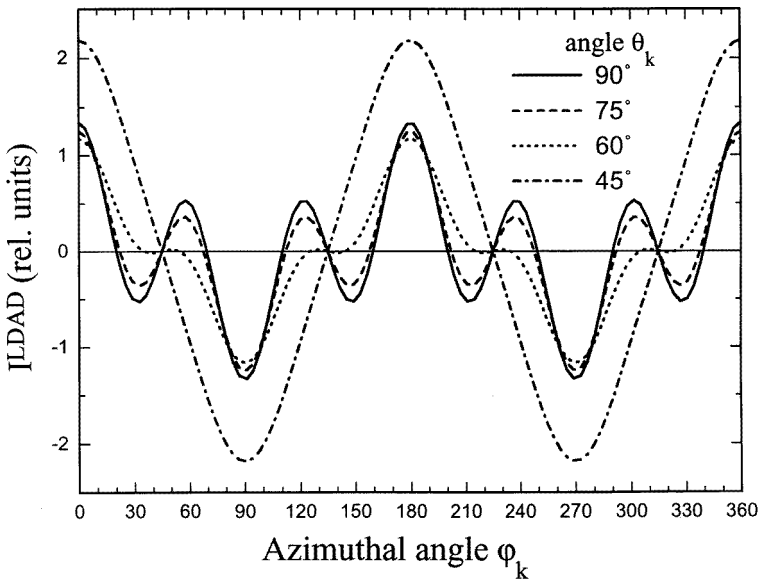

Figure 8. I^{LDAD} (the term in square brackets of equation (19)) as a function of φ_k for different angles θ_k. As in figure 3, the light is incoming along the C_4 rotation axis.

It is also worth mentioning that, in agreement with the general discussion presented in [26, 27], the LDAD is proportional to terms containing the real part of the products of transition moments that corresponds to the cosine of the phase-shift differences, whereas the CDAD is proportional to the imaginary part of those products and corresponds to the sine of the phase-shift differences. Therefore, CDAD and LDAD measurements give complementary information and together can unambiguously define this phase-shift difference, including its sign.

For molecules fixed in space one can derive also the linear dichroism (LD) which is obtained from the general expression (14) for the LDAD by integration over the ejection angles of photoelectrons:

$$\begin{aligned}\mathrm{LD}(\boldsymbol{q}) = \frac{\sigma_k(E)}{B}\Big\{&[|\langle 0|z|^a F^1_{10}\rangle|^2 + |\langle 0|z|^a F^1_{11}\rangle|^2 + |\langle 0|z|^a F^1_{12}\rangle|^2 + |\langle 0|z|^a F^1_{13}\rangle|^2 \\ &-\frac{1}{2}[|\langle 0|x|^e F^1_{11}\rangle|^2 + |\langle 0|y|^e F^2_{11}\rangle|^2 + |\langle 0|x|^e F^1_{12}\rangle|^2 + |\langle 0|y|^e F^2_{12}\rangle|^2 \\ &+|\langle 0|x|^e F^1_{13}\rangle|^2 + |\langle 0|y|^e F^1_{13}\rangle|^2 + |\langle 0|x|^e F^1_{23}\rangle|^2 + |\langle 0|y|^e F^2_{23}\rangle|^2] \\ &+\cdots]\sin^2\theta_q\cos(2x_q)\Big\}. \end{aligned} \tag{20}$$

The general structure of this expression is the same as that for linear molecules though the dynamical part of (20) contains also the terms with the transition moments specific for C_{4v} molecules. Such an expression can be useful for experiments with molecules in a gas phase oriented by an external field or by rapid dissociation that follows the ionization process [36].

5. Conclusions

We investigated theoretically the properties of angular distributions of photoelectrons (ADP) for adsorbate–substrate systems fulfilling C_{4v} local symmetry or for molecules of the same symmetry fixed in space. The cross section expressions were obtained using the continuous spectrum wavefunctions expanded in symmetry-adapted harmonics [15] instead of the standard spherical harmonics used previously. The main advantage of this approach is the possibility of obtaining relatively simple analytical expressions for ADPs for electrons ejected by circularly or linearly polarized light with symmetry-adapted constraints taken into account. One will see the local symmetry behaviour in the differential cross section, CDAD and LDAD provided that the kinetic energy of the electron is such that the associated de Broglie wavelength is shorter than the dimension of the elementary cell of the surface. Usually this occurs above a few electron-volts of kinetic energy.

The present approach is an alternative language for the description of backscattering and diffraction of photoelectrons ejected from adsorbed species [11–14] as well as of the effects of chemical bonding of adsorbates with the substrate [6]. Here the backscattering is restricted to the surrounding atoms of the adsorption site included in the cluster and the whole calculation is done in one step. The periodicity of the surface is neglected.

However the model assumes that the local symmetry can be seen at the macroscopic level that corresponds implicitly to including periodicity and the electron diffraction from the neighbouring atoms of the adsorption site. In the backscattering model of [11–14] the calculations proceed in two steps: first the transition probability of adsorbed species alone is calculated. Then one obtains the collision probability between the photoelectron and the atoms of the surface. The two results are brought together through a photoelectron diffraction model (see for example Sebilleau *et al* [13a]). For an O atom adsorbed on a Cu(100) surface [13b], one obtains by this method a $\sin(4\varphi_\kappa)$ behaviour for the CDAD in agreement with the results obtained in the present paper.

To unravel the characteristic symmetry properties of the ADP, the absorption of light propagating along the C_4 rotation axis was investigated as a function of the azimuthal angle φ_κ. We obtained explicit formulae for ADPs for linearly and circularly polarized light for ℓ restricted to the maximum value of 3. Most clearly the fourfold symmetry of C_{4v} molecules reveals itself for absorption of circularly polarized light when the ADP contains only terms proportional to $\cos(4m\varphi_\kappa)$ and $\sin(4m\varphi_\kappa)$, $m = 0, 1, 2\ldots$ ($m = 0, 1$ provided that $\ell \leqslant 3$; $m = 0, 1, 2\ldots$ otherwise). The CDAD under the same conditions is proportional to $\sin(4m\varphi_\kappa)$, $m = 1, 2, \ldots$. For linearly polarized light the ADP has a rather complicated dependence on the azimuthal angle φ_κ containing terms proportional to $\cos(2m\varphi_\kappa)$, $m = 0, 1, 2, \ldots$. In LDAD the contribution of terms containing $\cos(2m\varphi_\kappa)$ with even m, $m = 0, 2, 4\ldots$ cancels out and no clear fourfold symmetry appears. This difference between circularly and linearly polarized light is connected with the symmetry of the light beam. Circularly polarized light has no characteristic direction in the surface plane, therefore the symmetry properties of the surface are revealed in the angular distribution. Linearly polarized light has a characteristic direction in the surface plane given by the polarization vector $\boldsymbol{e}$, that leads to the appearance of terms in the angular distributions having a symmetry other than fourfold.

In the numerical simulation discussed above we had in mind the adsorption of $c(2 \times 2)$ CO molecules on a Ni(100) surface, but the equations obtained here can be used for molecules of C_{4v} symmetry group fixed in space, for adsorbed atoms or linear molecules when the adsorption site has C_{4v} symmetry and for photoemission from clean surfaces having C_{4v} symmetry. The general properties of the angular distributions discussed above

can be observed in experiments of the type presented in [37], in which the photoemission from a clean Si(001) surface over a cone of half-angle 45° about the surface normal was investigated.

For different symmetry groups the ADP will have different symmetry properties, which can be used to establish the local symmetry of the adsorbate–substrate system and to differentiate the adsorption sites, as is usually done using an internal vibrational mode of the adsorbate in infrared spectroscopy [38]. With increasing coverage new adsorption sites can be populated, or as the lateral interactions between molecules become stronger the adsorbates appear to be tilted about the surface normal. The problem of coverage was treated recently [33] for the CO/Ar(100) system using a classical mechanics dynamical model showing that the precession about the surface normal is destroyed when the coverage is increased. Investigating the dependence of the ADP on the azimuthal angle φ_κ with increasing coverage can be used to unravel the modification of the local symmetry of the adsorbate–substrate system. Of course, the fact that adsorbed molecules are tilted can be discovered by the symmetry arguments only if they are all tilted in the same direction. Otherwise the result of observation will correspond to averaging over several equivalent adsorption sites with different azimuthal directions of tilting angle, giving a pattern of the same symmetry as if the molecules were standing upright. Alternatively, photoelectron diffraction at moderate kinetic energies can be used to investigate the symmetry of the local adsorption site (see the reviews [39, 30]). One wonders whether the distinction between the adsorption sites can be observed also for low kinetic energies of the ejected electrons. Our theoretical model that is independent of energy seems to show that corresponding experiments are possible.

As discussed in section 1, we have neglected the vibrational motion of the adsorbate, particularly the hindered rotation [29]. The nuclear motion can destroy the local symmetry of the adsorbate–substrate system and smear out the symmetry patterns which one should normally see in the spectra. Also the mean angle of orientation of the internuclear axis can be tilted and the molecule can precess about the surface normal. Experimentally, for CO on Ni(111) or on Pd(111) [30, 31], this angle is 5–15° but it has also been estimated to be up to 30° by LEED [32]. Because the required energy is low, for very small tilting angles one can assume that the adsorbed site symmetry is conserved. For larger angles and no precession about the surface normal, the local symmetry of the adsorbate surface complex is lower than the symmetry of the adsorption site itself.

Finally, note that we show here that the local symmetry of the adsorption site generated in the transition moments gives rise to characteristic oscillations in the cross section and dichroism. Observing such oscillations in the spectrum does not necessarily imply a particular symmetry of the adsorption site. It can happen that the adsorbed atoms or molecules occupy an off-symmetry position relative to the substrate. Several equivalent off-symmetry positions of that type can be occupied with equal probability. In experiments photoelectrons are usually collected from a relatively large area and the observed picture will correspond to averaging over these several equivalent positions, leading to a high symmetry of the spectra. Evidently, in that case one could not distinguish between a really symmetrical adsorption site and the average of several equivalent off-symmetry sites. To prove a local or global interpretation one should compare several experimental techniques (such as photoelectron diffraction and/or LEED) and theoretical models. For a given experimental method the rough data cannot be interpreted without some theoretical modelling that can be simple (usually done by the experimentalists themselves) or more sophisticated.

Acknowledgments

VVK acknowledges the Grant Centre of St Petersburg University for financial support. He also acknowledges the Laboratoire de Photophysique Moléculaire du CNRS for the hospitality extended to him during a 3 month stay in the framework of a 'Contrat de Cooperation CNRS entre la France et la Russie' when a part of this work was performed. NAC acknowledges the hospitality of the Johannes Gutenberg Universität Mainz extended to him during the work on this paper and the financial support of the Deutsche Forschungsgemeinschaft through SFB 252.

References

[1] Smith R J, Anderson J and Lapeyre G J 1976 *Phys. Rev. Lett.* **37** 1081
[2] Dill D 1976 *J. Chem. Phys.* **65** 1130
[3] Dill D, Siegel J and Dehmer J L 1976 *J. Chem. Phys.* **65** 3158
[4] Davenport J W 1976 *Phys. Rev. Lett.* **36** 945
[5] Cherepkov N A and Kuznetsov V V 1987 *Z. Phys.* D **7** 271
[6] Gadzuk J W 1974 *Phys. Rev.* B **10** 5030; 1975 *Phys. Rev.* B **12** 5608
[7] Schichl A, Menzel D and Rösch N 1984 *Chem. Phys. Lett.* **105** 285
[8] Dubs R L, Smith M E and McKoy V 1988 *Phys. Rev.* B **37** 2812
[9] Budau P, Büchner M and Raseev G 1993 *Surf. Sci.* **292** 67
[10] Budau P and Raseev G 1995 *Phys. Rev.* B **51** 16 993
[11] Liebsch A 1974 *Phys. Rev. Lett.* **32** 1203; 1976 *Phys. Rev.* B **13** 544
Pendry J B 1975 *J. Phys. C: Solid State Phys.* **8** 2413
[12] Herbst J F 1977 *Phys. Rev.* B **15** 3720
[13] (a) Sebilleau D, Treglia G, Desjonqueres M J, Spanjaard D, Guillot C, Chauveau D and Lecante J 1988 *J. Physique* **49** 227
(b) Budau P and Stan G 1995 *Surf. Sci.* **331–333** 1213
(c) Fadley C S 1992 *Synchrotron Radiation Research: Advances in Surface and Interface Science, Volume 1: Techniques* ed R Z Bachrach (New York: Plenum) ch 9
[14] Fecher G H 1995 *Europhys. Lett.* **29** 605
[15] Burke P G, Chandra N and Gianturco F A 1972 *J. Phys. B: At. Mol. Phys.* **5** 2212
[16] Chandra N 1987 *J. Phys. B: At. Mol. Phys.* **20** 3405; 1989 *Phys. Rev.* A **40** 752
[17] Cherepkov N A and Kuznetsov V V 1991 *Phys. Rev.* A **44** 2220
[18] Reid K L and Powis I 1994 *J. Chem. Phys.* **100** 1066
[19] (a) Andersson S and Pendry J B 1978 *Surf. Sci.* **71** 75
(b) Allyn C L, Gustafsson T and Plummer E W 1978 *Solid State Commun.* **28** 85
(c) Horn K, Bradshaw A M and Jacobi K 1978 *Surf. Sci.* **72** 719
(d) Rieger D, Schnell R D and Steinmann W 1984 *Surf. Sci.* **143** 157
(e) Uvdal P, Karlsson P A, Nyberg G, Andersson S and Richardson N Y 1988 *Surf. Sci.* **202** 167
[20] Cherepkov N A 1982 *Chem. Phys. Lett.* **87** 344
[21] Dubs R L, Dixit S N and McKoy V 1985 *Phys. Rev. Lett.* **54** 1249; 1986 *J. Chem. Phys.* **85** 656, 6267
[22] Schönhense G 1990 *Phys. Scr.* T **31** 255
[23] Cherepkov N A 1994 *Adv. At. Mol. Opt. Phys.* **34** 207
[24] Westphal C, Bansmann J, Getzlaff M, Schönhense G, Cherepkov N A, Braunstein M, McKoy V and Dubs R L 1991 *Surf. Sci.* **253** 205
Bansmann J, Ostertag Ch, Getzlaff M, Schönhense G, Cherepkov N A, Kuznetsov V V and Pavlychev A A 1995 *Z. Phys.* D **33** 257
[25] Chandra N 1989 *Phys. Rev.* A **39** 2256
[26] Cherepkov N A and Schönhense G 1993 *Europhys. Lett.* **24** 79
[27] Cherepkov N A and Raseev G 1995 *J. Chem. Phys.* **103** 8238
[28] Ostertag Ch, Bansmann J, Grünewald Ch, Jentzsch Th, Oelsner A, Fecher G H and Schönhense G 1995 *Surf. Sci.* **331–333** 1197
[29] Büchner M and Raseev G 1994 *Phys. Rev.* B **49** 2768
[30] Plummer E W and Eberhardt W 1982 *Adv. Chem. Phys.* **49** 533
[31] Miranda R, Waldelt K, Rieger D and Schnell R D 1984 *Surf. Sci.* **139** 430

[32] Van Hove M A, Weinberg W H and Chan C-M 1986 *Low-Energy Electron Diffraction* (New York: Springer) p 309
[33] Parneix P, Büchner M, Raseev G and Halberstadt N 1995 *Chem. Phys. Lett.* **233** 430
[34] Raseev G, Giusi-Suzor A and Lefebvre-Brion H 1978 *J. Phys. B: At. Mol. Phys.* **11** 2735
Raseev G 1980 *Comput. Phys. Commun.* **20** 275
[35] Altmann S L 1957 *Proc. Camb. Phil. Soc.* **53** 343
Altmann S L and Bradley C J 1963 *Phil. Trans. R. Soc.* A **255** 199
[36] Guyon P M, Golovin A V, Quayle C J K, Vervloet M and Viard M R 1996 *Phys. Rev. Lett.* **76** 600
[37] Daimon H, Nakatani T, Imada S, Suga S, Kagoshima Y and Miyahara T 1993 *Japan. J. Appl. Phys.* **32** L1480
Kaduwela A P, Xiao H, Thevuthasan S, Fadley C S and Van Hove M A 1995 *Phys. Rev.* B **52** 14 927
[38] Persson B N J, Tüshaus M and Bradshaw A M 1990 *J. Chem. Phys.* **92** 5034
[39] Woodruff D P and Bradshaw A M 1994 *Rep. Prog. Phys.* **57** 1029